Proceedings of ASME Turbo Expo 2011
GT2011
June 6-10, 2011, Vancouver, British Columbia, Canada

GT2011-46639

CAN-ANNULAR COMBUSTION CHAMBER SURFACE TEMPERATURE MEASUREMENTS AND DAMAGE SIGNATURES AT OPERATIONALLY REPRESENTATIVE CONDITIONS

D. Bouchard, G. Pucher and W.D.E. Allan
Royal Military College of Canada
Kingston, Ontario, Canada K7K 7B4

ABSTRACT

An experimental program which investigated the surface temperature distribution of a contemporary gas turbine combustion liner is presented. An array of 65 embedded surface mounted thermocouples was installed on a Rolls Royce/Allison T56 combustion liner and exposed to combustion conditions in the Combustion Chamber Sector Rig (CCSR) at the Royal Military College of Canada. The CCSR was operated at two test points to simulate idle and cruise modes of operation. Corresponding exhaust temperature measurements were taken in the test combustion chamber exhaust plane with a sweeping thermocouple rake.

These efforts were the latest in a multi-year program to investigate the impact of service wear related geometric deformations of combustion liners and damaged/fouled fuel nozzles on the exit temperature profile from typical combustion chambers. It has been previously ascertained that real-world geometric anomalies in the T56 combustion chambers, particularly in the transitional zone, can modify the exhaust temperature profile to a sufficient degree so as to risk hot section damage due to excessive heat exposure. The collection and analysis of surface temperature data represents a useful extension of the knowledge base of the T56 combustion system within the context of the overall program and is paramount to upcoming numerical modelling efforts aimed at assessing hot section damage risks.

NOMENCLATURE

CCSR – Combustion Chamber Sector Rig
RMC – Royal Military College of Canada
CAF – Canadian Air Force
PF – Pattern Factor
TPTT – Thermal Paint Temperature Technology
Ma – Mach Number
CAD – Computer Aided Design
NGV – Nozzle Guide Vane
EGT – Exhaust Gas Temperature

BACKGROUND

The Canadian Air Force (CAF) aircraft fleet includes a significant number of Hercules CC-130 and Aurora CP-140 aircraft, which are powered by Rolls Royce/Allison T56 turboprop engines. Within the majority of these engines, the can-annular T56-A-15 Series III type combustion liner serves to burn fuel and power the hot (turbine) section of the engine. Figure 1 shows a cutaway of the T56-A-15 engine. Six combustion liners are distributed radially upstream of the turbine section. Figure 2 shows a cutaway of the Series III combustion chamber with details of the various sections including the primary, secondary and dilution regions.

The limiting of peak temperatures of hot gases emerging from combustion liners is paramount to the avoidance of turbine section damage. Even within the confines of a liner without any geometric flaws and with a nozzle functioning to specification, a non-uniformity of the exhaust plane temperature field exists. This phenomenon is often quantified by a calculated parameter based on exhaust plane temperatures called Pattern Factor (PF) which will be discussed further in the results section. Elevated PF values represent an increased risk of hot section damage.

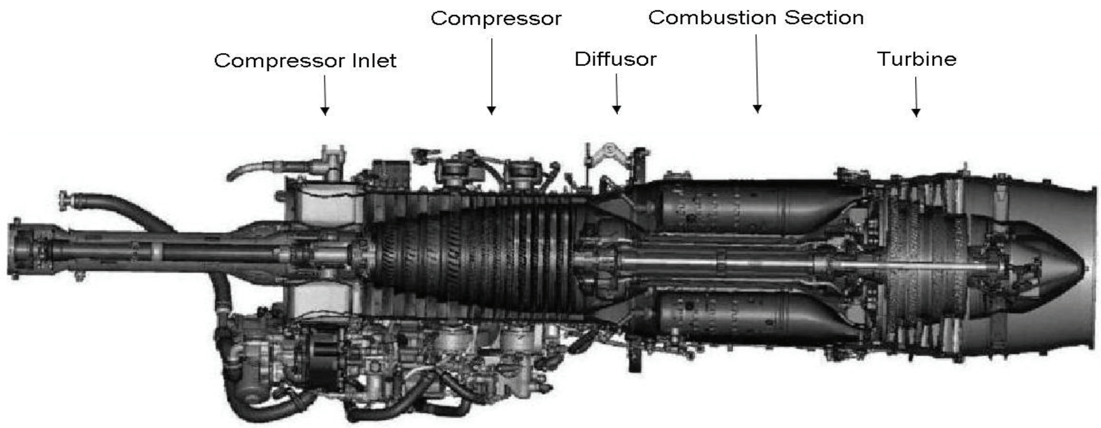

Figure 1: Cutaway Schematic of the T56-A-15 Turboprop Engine

The efforts and results described in this paper are the latest in a research program sponsored by the CAF at the Royal Military College of Canada (RMC) to investigate the impact of geometric deformations of combustion liners and damaged fuel nozzles on the exit temperature distribution from the T56 combustion chamber. It has been previously ascertained that real-world geometric anomalies do exist in the can-annular liners, artifacts of design and exacerbated by in-service use. These temperature exceedances tend to occur particularly in the transitional section of the liners and can modify the exhaust temperature profile to a sufficient degree to risk hot section damage due to excessive heat exposure [1,2]. RMC explored the geometric contributions using a laser scanner to quantify geometric deviations for a population of Series III liners against a baseline non-damaged liner.

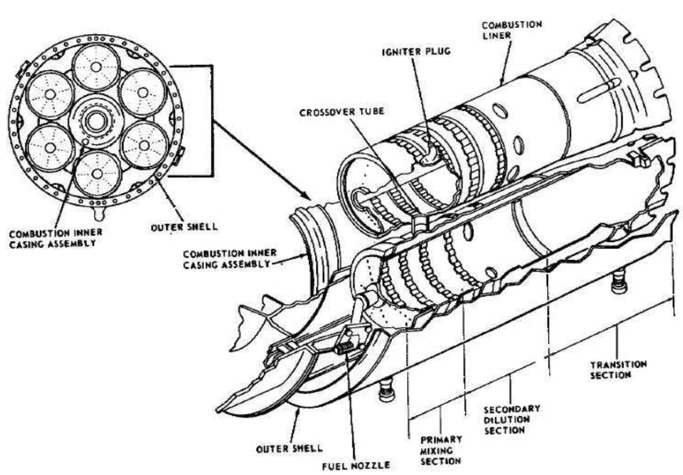

Figure 2: Details of the T56-A15 Series III Combustion Chamber [3]

By correlating these deviations to corresponding PF values obtained through combustion tests on the CCSR, it was determined that small deviations from stock dimensions within the dilution zone can cause a significant increase in PF. A decrease in the mixing of the products of combustion in the dilution zone was also correlated to dilution zone damage or geometric deviation from stock. Figure 3 shows the summary of PF vs Standard Deviation of geometric deviation in the dilution zone from the study.

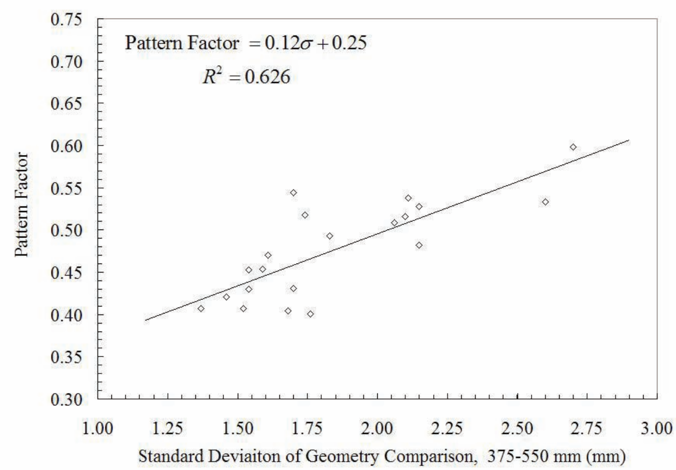

Figure 3: Correlation of Fishmouth Geometry Deviation to Pattern Factor [2]

In the second phase of the study relating nozzle condition to exhaust temperature profile [3], it was also shown that faults in the spray pattern translated into detrimental effects on PF. Within this project, the impact of nozzle faults on liner surface temperatures was investigated. As such, a thermal paint which responds to peak temperature conditions was applied to a liner before exposure to combustion conditions within the CCSR with both a serviceable and unserviceable nozzle. Figure 4 shows the results of this investigation, where a distinct difference was noted in liner surface temperature distributions for the two nozzles investigated. It was found that the serviceable nozzle with a uniform spray distribution produced a more symmetrical temperature distribution about the centreline for the outer radius of the liner. Notwithstanding for the inner radius (Figure 4), the serviceable nozzle produced a larger more uniform intermediate temperature region (745 K) than the unserviceable nozzle, but similar higher temperature (1161 K) regions to the unserviceable nozzle. The obvious implications were that just as the potential exists for hot section damage when liners and/or nozzle are damaged due to flow and heat transfer modifications, the same can be true for liner surfaces themselves in regions where higher temperature concentrations exist.

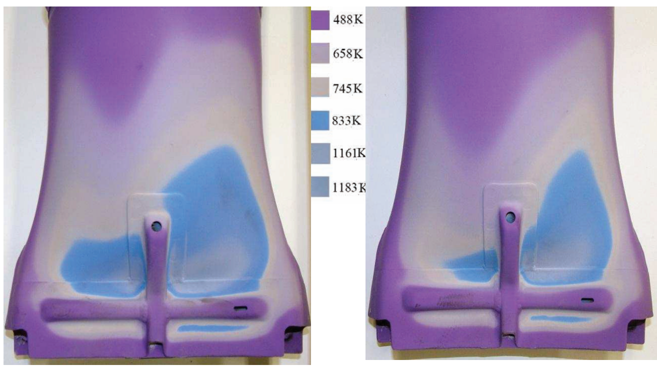

Figure 4: Inner Radius for a) Serviceable Nozzle and b) Unserviceable Nozzle [3]

In a comprehensive study performed by Rizk et al., the impact of high density fuels on T56 combustion liner was investigated using thirty surface mounted thermocouples [4]. Differences in the temperature distribution were then observed for the different fuel types investigated, with higher temperatures seen in the transition section of the liner. It was also concluded that liner thermal loading as a function of fuel type was directly related to fatigue life due to localized stress concentrations.

In order to perform numerical predictions of turbine inlet section hot spots resulting from liner geometry imperfections, a database of liner surface temperature distribution is essential for a variety of service-exposed liners. In the current experimental study, the majority of the 65 surface-mounted thermocouples were situated in the transition zone. The CCSR was then operated at matched idle and cruise conditions and corresponding exhaust temperature data were recorded using the thermocouple rake. The relative uniformity of surface temperature in the transition zone was related to the exhaust PF for the operating conditions. Comparisons were made with a qualitative combustion chamber surface temperature distribution facilitated using thermally sensitive paint. Further efforts in this study will involve the instrumentation of damaged T-56 combustion liners with surface mounted thermocouples.

EXPERIMENTAL

Liner Thermocouple Installation

To assist in the selection of the locations for thermocouples to be mounted on the T56-A-15 combustion liner, a thermal paint was applied to the liner. This Thermal Paint Temperature Technology™ (TPTT) paint is temperature sensitive and renders an irreversible representation of maximum temperatures sustained on surfaces through a distinct colour coding scheme. After painting and curing the liner according to the specified procedure, it was exposed in the CCSR to the matched cruise operating condition. Images of the resulting colour patterns are found in the results section.

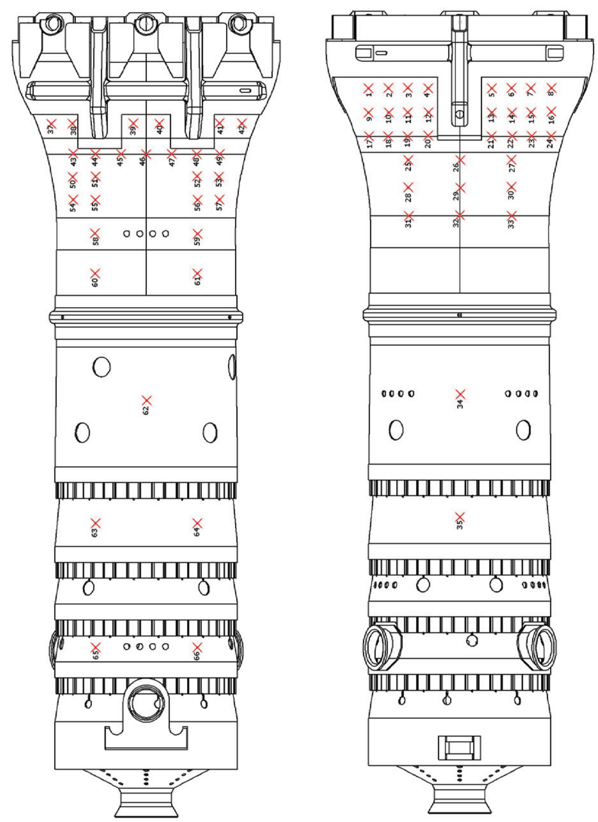

Figure 5: Thermocouple Locations (Depicted by *X* symbols) on the T56-A-15 Liner

A total of sixty-five exposed-junction K-type thermocouples with a sheath diameter of 0.813 mm (0.032″) were installed on the surface of the test combustion chamber. A rotary cutting tool cut channels to a depth equaling one half (0.635 mm) of the thickness of the combustion liner skin. The initial plan had been to use silver solder to braze the thermocouples in place and a discarded liner was used to establish an appropriate procedure. It was determined that this methodology, would result in an unacceptably low thermocouple survival rate, so another means of mounting the probes on the liner surface was sought. A nickel-based metallic adhesive was attempted. This compound was able to sustain a temperature to 1100ºC [6]. A location map for the thermocouple probes was developed, based upon the surface thermal paint colour scheme observed on the liner following the CCSR test, in conjunction with observations from Bishop regarding locations of highest thermal loading, as seen in Figure 4 [3]. This map is shown in Figure 5.

After the thermocouples were installed, the instrumented liner was carefully transferred to the CCSR and extension wires were installed with high temperature ceramic connectors. These wires exited the rig via unused fuel nozzle ports in the inlet section of the CCSR. During tests, the temperature signals from the surface mounted thermocouples were measured with portable data loggers at a frequency of 1 Hz. The Labview ™ based control and monitoring system of the CCSR recorded relevant data including fuel flow, rig operating temperatures and pressures, and exhaust rake temperatures.

COMBUSTION CHAMBER SECTOR RIG

The CCSR which was jointly designed by the RMC and StandardAero has served in various experimental programs related to the Rolls Royce/Allison T56-A-15 combustion systems. In addition to the efforts described above related to liner and nozzle defects [1,2,3], synthetic fuel and additive performance has been evaluated with the CCSR [5].

While the combustion systems within the rig comprise actual T56 components, the inlet, air delivery and fuel systems are custom designs. The T56 combustion liner is of can-annular design and there are six per engine. Within the CCSR, only one liner supports combustion, while the radially adjacent liners serve to provide the active liner with a more realistic airflow simulation. Figure 6 shows the CCSR in a partially disassembled state revealing the instrumented operational (centre) and neighbouring liners.

A *quasi non-dimensional Mach number,* as described in Equation 1, was used to match inlet flow conditions of the rig, relative to the real engine operating conditions. The values of these parameters where chosen such that the calculated value of the quasi non-dimensional Mach number matched that for an in-flight cruise condition, using a methodology described by Jermy et al. [7].

$$\hat{Ma} = \frac{\dot{m}_{air}\sqrt{T_3}}{P_3} \qquad (1)$$

Table 1 lists the values of the air mass flow rates and the combustion chamber inlet temperatures and pressures for the T56 engine and the CCSR.

Table 1 Inlet conditions for the engine and the CCSR

	Engine Setting	$\dot{m}_a$ [kg/s]	T3 [K]	P3 [kPa]
Engine	Idle	1.473	442	365
	Cruise	1.541	554	464
Rig	Idle	0.51	305	105
	Cruise	0.47	305	105

To account for the heat release effects on the combustion aerodynamics of the CCSR, the Equivalence ratio and the fuel droplet size were also matched to the in-flight cruise conditions of the T56. This compensated for the non-pressurized, atmospheric conditions of the CCSR [8]. To facilitate the replication of in engine fuel spray characteristics (spray pattern and droplet Sauter Mean Diameter) while satisfying the requirement of reduced fuel flow for the test rig, the T56 nozzle used was modified by blocking the secondary flow circuit. A previous study ascertained that this technique provided satisfactory results [8]. Thus, despite significant differences in airflow, temperature, and pressure, a flow similitude is achieved between rig and engine, in terms of Mach number, Equivalence ratio and fuel droplet size. Reynolds number is not matched, but is sufficiently high to be of secondary importance [3,8,9,10,11,12,13].

Given that the air flow through the active combustion liner in the CCSR rig was much lower than that of a pressurized in-flight liner, a much lower fuel flow was also required. As such, a T56 fuel nozzle was modified by blocking its secondary flow circuit. This test nozzle performance was verified to produce a fuel droplet size distribution and cone angle which closely simulated an unmodified nozzle in an in-flight operation [8]. A target equivalence ratio of 0.23 was chosen for tests. For the idle simulation, an equivalence ratio of 0.146 and a mass airflow of 0.5 kg/s were selected to satisfy parameters of Equation (1). A stepper motor-controlled water cooled sweeping rake, which itself housed 4 K-type thermocouples was used to scan the 2-dimensional sector shaped exit plane (*fishmouth*) to determine temperature maps within a 1 degree resolution. This rake is shown in Figure 7.

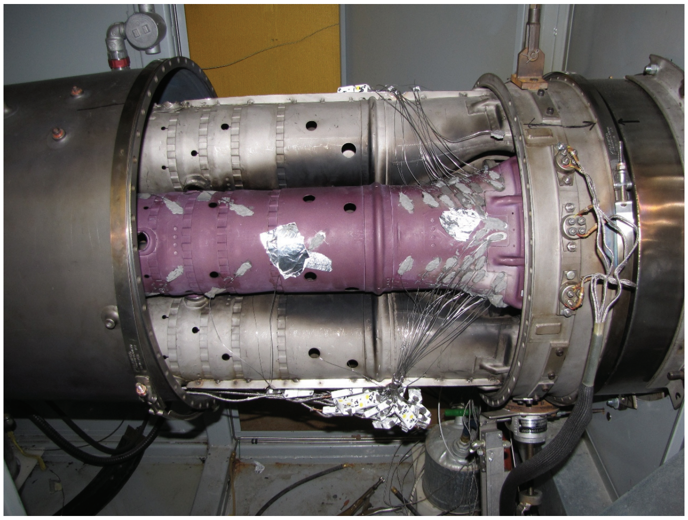

Figure 6: Partially Disassembled Combustion Chamber Sector Rig (CCSR) Revealing the Main and Adjacent 'Dummy' Combustion Liners

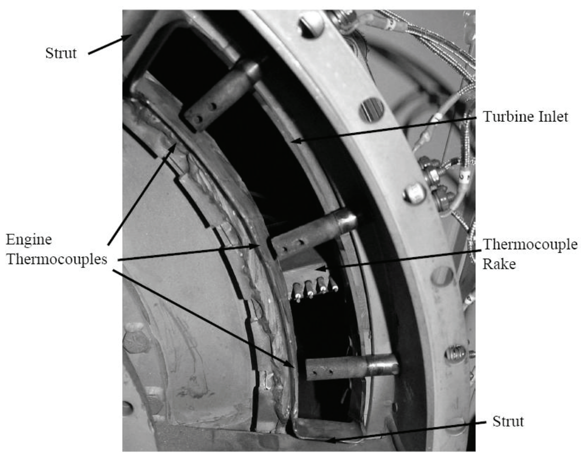

Figure 7: Thermocouple Rake Within the CCSR Rig

RESULTS

Thermal Paint Evaluation

Thermal paint was applied to the test combustion liner to map the surface temperature distribution and to provide information to assist in determining appropriate liner wall thermocouple positions. Figure 8 shows the transition and fishmouth regions of the liner, where the paint demonstrated colour changes indicating the highest surface operating temperatures. Figure 8(a) shows the highest overall temperature zones, which are distributed more symmetrically than those on the lower surfaces as seen in Figure 8(b). The scale relating the paint shade to temperature bins is also shown in the figure. The equivalence ratio used in the CCSR to generate these images was lower (0.23) than that used by Bishop (0.28) [3]. In her research, shades corresponding to higher temperatures were observed (Figure 4 reproduced from [3]). However, the asymmetrical nature of the temperature distribution between the studies was consistent.

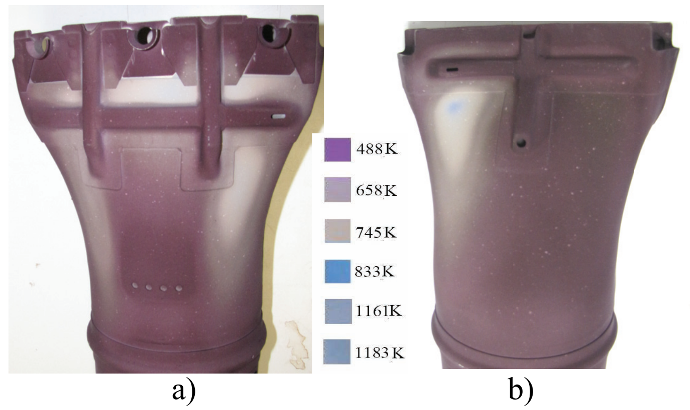

Figure 8: Thermal Paint Results, Depicting the Liner Temperatures of the a) Upper and b) Lower Surfaces of the test Combustion Can at Matched Cruise Operating Conditions

Combustion Liner Temperature

Four tests were performed in the CCSR to evaluate surface temperature trends on the T56 liner. These consisted of three operating points (two cruise and one idle), and a sensitivity analysis of surface temperatures to controlled deviations in air mass flow rate and equivalence ratio. In the course of experimentation, temperature data were logged continuously and the values extracted for analysis were selected while CCSR operation was stable at target conditions. Surface temperatures were found to be constant at such times.

To assist in the visualization of the combustion chamber liner wall temperature distribution, a series of thermal contour plots was developed. The surface thermocouple coordinates were coupled with the time averaged liner wall temperatures provided from the CCSR tests to produce these images. The Unix-based program *Gnuplot* was used to develop a two dimensional thermal contour plot projected onto the liner transition zone. The contour plot was then interlaced with the surface of a three dimensional CAD representation of the liner using *SolidWorks 2010*. These contour plots provide a higher degree of resolution than that offered by the thermal paint. Contour plots were not generated for the liner surface regions corresponding to the primary, secondary and dilution zones, due to the absence of strong thermal gradients.

From the cruise simulation tests, Figures 9 and 10 show the liner wall temperature contour plots of the transition zone, for the outboard and inboard surfaces, respectively. The temperature values from the two cruise condition trials were averaged in the generation of these plots. The transition zone experienced wall temperatures which ranged from 438 K to 886 K. The maximum temperatures were measured on the inboard surface. In Figure 9, an angular designation is introduced to assist the reader in anchoring spatial coordinates on the liner. When looking downstream with the outboard liner surface facing up, the 0° position is at the left side of the fishmouth, while the 60° position is at the right, as indicated in Figure 9.

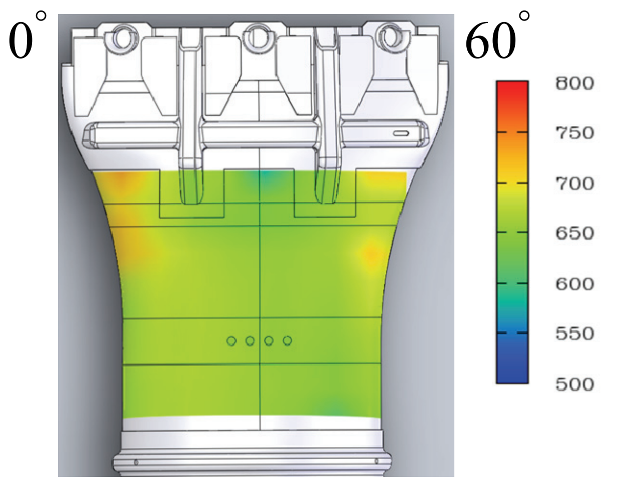

Figure 9: Liner Wall Temperature (K) Contours of the Outboard Surface While Operating at Cruise Conditions

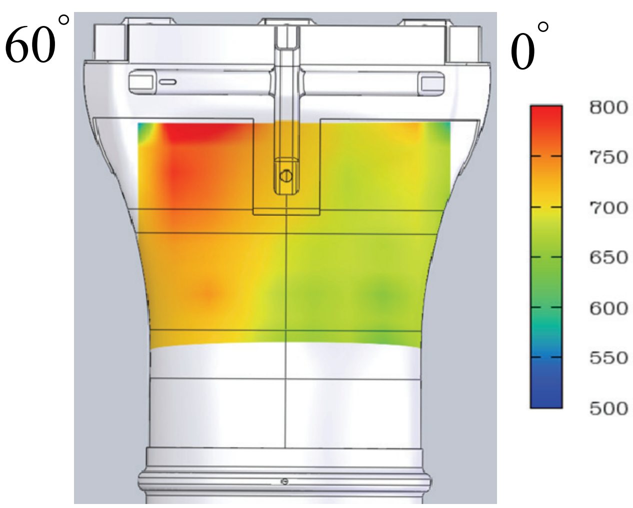

Figure 10: Liner Wall Temperature (K) Contours of the Inboard Surface while Operating at Cruise Conditions

Similar to Figures 9 and 10, Figures 11 and 12 represent the liner wall temperature maps for the idle operating condition. The thermal gradient trends shown in these figures are consistent with those from the cruise operating condition. In comparing the contour plots, it is noted that the regions of highest temperature are further downstream for the cruise condition, relative to the idle condition, particularly on the inboard surface. It is hypothesized that the relatively higher momentum of the gas in the cruise condition resulted in increased heat transfer further downstream towards the fishmouth due to higher fluid velocities.

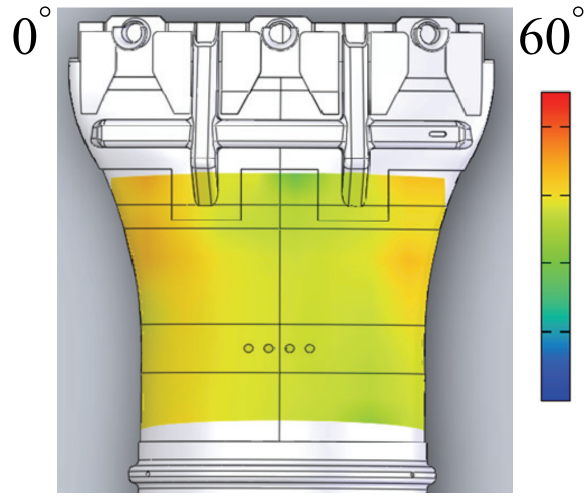

Figure 11: Liner Temperature (K) Contours of the Top Surface While Operating at the Idle Condition

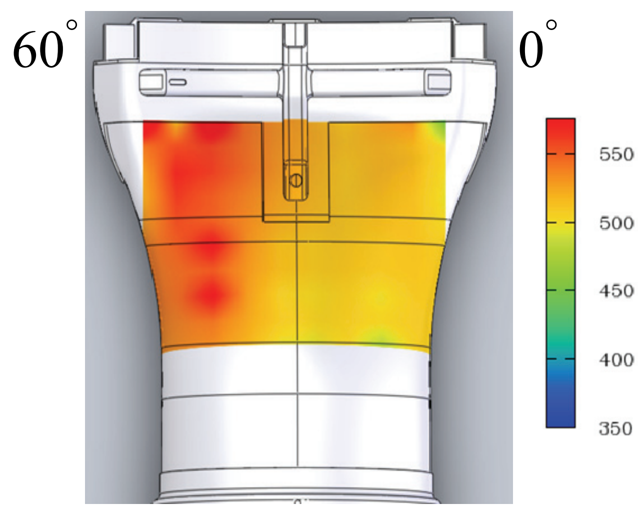

Figure 12: Liner Temperature (K) Contours of the Bottom Surface while Operating at the Idle Condition

EXHAUST PATTERN FACTOR

Figure 13 shows the two dimensional efflux gas temperatures obtained from the thermocouple traverse rake at the cruise and idle operating conditions in the CCSR. The contour plots demonstrate the variation in the gas temperature in the exit plane. The efflux gas temperature varied from 310-1622 K for the cruise condition and 315-980K for the idle condition. The temperature resolution in Figure 13 is 100 K. The average temperature of the exhaust was determined to be 1114K for cruise and 729K for idle. From a qualitative inspection, both figures suggest that the temperatures of gas exiting the 60° side of the combustion can are generally greater than the 0° side. This is consistent with the hotspots observed in Figures 10 and 12, showing that on the inboard surface of the liner, the average temperature increases in traversing from 0 to 60°.

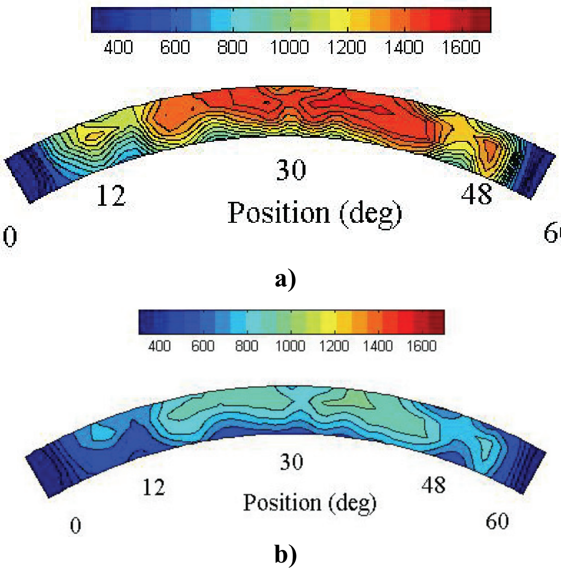

Figure 13: The Efflux Gas Temperature Contours Obtained from the Traverse Rake at a) Cruise Condition and b) Idle Condition

The exhaust PF gives a relative measure of the thermal uniformity of the efflux gas and is defined by the following equation [1,2,3,12]:

$$PF = \frac{T_{max} - T_{mean}}{T_{mean} - T_{inlet}}$$

A PF reduction represents an increase in the relative uniformity of temperature distribution and vice versa. Excessive PF values can correlate to an increased risk of turbine wear and damage due to the presence of local temperatures exceeding material limits. PF values of 0.60 and 0.59 were observed for cruise and idle conditions, respectively.

Liner to Exhaust Temperature Correlation

To explore whether the asymmetric temperature distribution observed on the liner surfaces could be related to the efflux gas temperature field, both parameters were graphically compared as a function of radial position, as described previously.

Figure 14 represents the correlation between the experimentally determined liner wall temperatures and the average efflux gas temperatures from the traverse rake. Figure 14 compares these temperatures to their respective position on the projected axial plane. The asymmetrical thermal gradient observed on the liner appears to translate downstream to the exiting gases, indicative of insufficient dilution zone cooling. It is hypothesized that the liner and gas temperatures showed an inverse relationship because regions of high heat transfer to liner surfaces resulted in lower exhaust temperatures and vice versa.

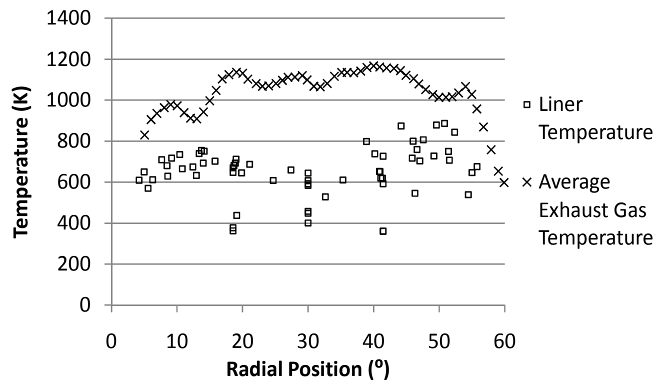

Figure 14: Radial Plot of Liner and Efflux Gas Average Temperature

To explore further whether the results shown in Figure 14 could be categorized to the outboard and inboard surfaces, the liner temperature data corresponding to the outboard surface were plotted with the top row of the thermocouple rake in Figure 15 and vice versa for Figure 16.

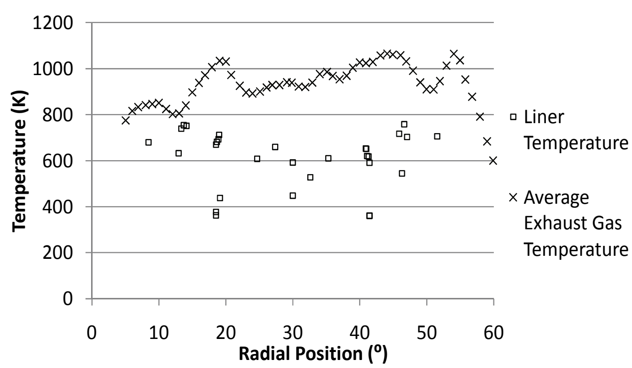

Figure 15: Radial Plot of Liner and Efflux Gas Temperatures for the Outboard Surface

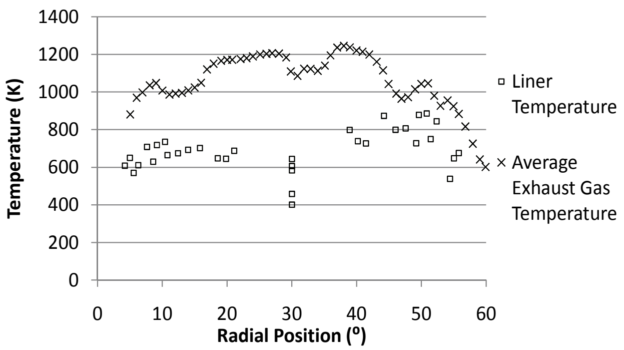

Figure 16: Radial Plot of Liner and Efflux Gas Temperature for the Inboard Surface

As compared to Figure 14, Figures 15 and 16 show improved correlations between liner surface temperatures and exhaust temperatures with Figure 16 showing a better correlation for the inboard surface. The apparent lack of correlations seen in Figure 15 is partly due to the less structured placement of the liner thermocouples. All liner thermocouple measurements are included in these two figures, including the thermocouples positioned in the primary, secondary and dilution zones. The liner thermocouples in the primary and secondary zones measured lower temperatures overall than the majority in the later portion of the dilution zone.

DISCUSSION AND CONCLUSIONS

There appears to be a significant amount of asymmetrical heat transfer occurring in the dilution zone. This characteristic flow asymmetrically heats the liner and is representative of insufficient dilution zone mixing. This occurrence is likely due to the seemingly random positioning of the dilution zone holes.

In the instrumentation process of the combustion liner, a number of thermocouples did not properly adhere to the liner surface. As a result, a few thermocouples became dislodged in the process of transporting and installing the test article into the CCSR. Minor thermocouple repairs were executed before operation; however a few thermocouples were unsuccessfully re-installed. As a result, there were a few locations that would have ideally contained more thermocouples; however due to the can geometry, the installation of thermocouples in these areas was found to be impractical. With this in mind, more thermocouples in these areas would have expanded the surface area of the liner wall temperature contour results, particularly the downstream regions approaching the fishmouth exit. For interpolated to produce finer contour plots. The assumption that the trend varies gradually with the radial and axial positions is reasonable given the nature of the combustion flow.

The two dimensional contour plots of liner wall temperature had a much finer resolution than those provided by the thermal paint (thermal paint ≈150 – 200 K, thermocouple contour plots ≈ 30 K). Nonetheless, the thermal paint provided a superior spatial resolution to the surface thermocouples and was invaluable in the selection of the thermocouple installation locations. By directly measuring the liner wall temperatures, a quantitative temperature assessment is provided, allowing for the interpolation of neighbouring wall temperatures.

The liner wall temperature data and analysis presented in this paper were relevant to the life and wear of both the turbine components and combustion liners. An assessment of the hotspot locations on the liner surface may provide an indication of corresponding radial peak exhaust gas temperature locations in the exhaust plane. Since the first engine component encountered downstream of the combustion chamber is the turbine, excessively high thermal stresses are known to erode NGVs. The NGVs are more susceptible to wear and creep than the turbine rotors since, unlike the rotors they are stationary and therefore continuously exposed to any local excessive temperatures. This phenomenon often goes unnoticed as the three EGTs sensors located in the fishmouth exhaust plane of each liner are electrically wired in parallel, and therefore only report the average efflux gas temperature, for all 18 EGTs in a T56 engine (3 EGTs per can). This regrettably masks hotspots.

The wall temperatures are significant to the life and reliability of the combustion liners. Continuous exposure to excess temperatures beyond material limits increases the tendency to creep. Up to this point combustion liner thermal degradation has not been to main area of focus of the experiments performed on the CCSR. The experimental data provided in this report exposed the existence of, and quantifies hotspots in a combustion liner void of defects. The magnitude of hotspots encountered with severely damaged nozzles and liners could potentially be much more severe. If a finite section is subject to a thermal loading beyond design limits, cyclic fatigue of the combustion liner and creep can lead to the deformation and cracking of combustion can geometry [14].

In comparing the two operating conditions matched: idle and cruise, a correlation is clear between the two cases. In both scenarios a distinct thermal gradient was present on side A of the lower region in the transition zone. This asymmetrical hot spot with respect to location on the T56 combustion liner is reported to exist not only as a consequence of CCSR operation, but also within actual T56 engines [9].

References

1. Kotzer, C., LaViolette, M. and Allan, W., “Effects of Chamber Geometry Upon Exit Temperature Profiles”, Proceedings of ASME Turbo Expo 2009: Power for Land Sea and Air, GT2009-60156, June 2009.
2. Kotzer, C., “Effects of Combustion Chamber Geometry Upon Exit Temperature Profiles”, Master’s Thesis, Royal Military College of Canada, April, 2008

3. Bishop, K.M., “Effects of Fuel Nozzle Condition Upon Gas Turbine Combustion Chamber Exit Temperature Profiles”, Master’s Thesis, Royal Military College of Canada, May 2009
4. Rizk, N.K., Oeschle, V.L., Ross, P.T. and Mongia, H.C., “High Density Fuel Effects”, Technical Report AFWAL-TR-88-2046, Wright Patterson Air Force Base, Aero Propulsion Laboratory, 1988.
5. Pucher, G., Allan, W., and Poitras, P., “Emissions from a Gas Turbine Sector Rig Operated with Synthetic Aviation and Biodiesel Fuel, Proceedings from ASME Turbo Expo 2010: Power for Land Sea and Air, GT2010-22494, June 2010.
6. Cotronics Corp, Product Literature Sheet: Durabon 952.
7. Jermy, M., Hussain, M, and Greenhalgh, D., 2003, “Operating Liquid-fuel Airblast Injectors in Low Pressure Test Rigs: Strategies for Scaling Down the Flow Conditions,” Measurement Science and Technology, 14, pp. 1151-1158.
8. Pucher, G. and Wang, G.., T56 Nozzle Investigation for Spray Pattern and Droplet Sizing. Department of Mechanical Engineering Technical Report, Royal Military College of Canada, 2006.
9. Guy, S.R.D., “Optical Patternation of Fuel Sprays in a Gas Turbine Combustion Chamber under Operationally Representative Flow Conditions”, M.A.Sc Thesis. Royal Military College of Canada. Kingston, Ontario, June, 2008.
10. Lefebvre, A.H., 1999, *Gas Turbine Combustion*, Taylor and Francis Group, pp. 206-208.
11. Saravanamuttoo, H., 1990, “Recommended Practices for Measurement of Gas Path Pressures and Temperatures for Performance Assessment of Aircraft Turbine Engines and Components”, Tech. Rep. AGARD-AR-245, Advisory Group for Aerospace Research and Development.
12. Guy, S. and Allan, W., 2006, “Scaling of a Gas Turbine Combustion Chamber Test Rig to Simulate Operating Conditions’, Combustion Institute/Canadian Section, Spring Technical Meeting, Waterloo, Ontario, pp. 4-1-4-6.
13. Taylor, D., 1999, “A Turbomatch Model of the Allison T56-A-15 Engine,” Tech. Rep. Preliminary Year Dissertation, Cranfield University School of Mechanical Engineering.
14. Gouws, J.J., 2007, “Combining a One Dimensional Empirical and Network Solver with Computational Fluid Dynamics to Investigate Possible Modifications to a Commercial Gas Turbine Combustor,” University of Pretoria, Pretoria, Master’s Thesis

